

Electrical control of reversible and permanent magnetization reorientation for magnetoelectric memory devices

Tao Wu (吴涛),^{1,a)} Alexandre Bur,¹ Kin Wong,² Ping Zhao,¹ Christopher S. Lynch,¹ Pedram Khalili Amiri,² Kang L. Wang,² and Gregory P. Carman¹

¹Department of Mechanical and Aerospace Engineering, University of California, Los Angeles, California 90095, USA

²Department of Electrical Engineering, University of California, Los Angeles, California 90095, USA

(Received 1 March 2011; accepted 9 June 2011; published online 30 June 2011)

We report giant reversible and permanent magnetic anisotropy reorientation between two perpendicular easy axes in a magnetoelectric polycrystalline Ni thin film and (011) oriented $[\text{Pb}(\text{Mg}_{1/3}\text{Nb}_{2/3})\text{O}_3]_{(1-x)}\text{-}[\text{PbTiO}_3]_x$ (PMN-PT) heterostructure. The PMN-PT is partially poled prior to Ni film deposition to provide a remanent strain bias. Following Ni deposition and full poling of the sample, two giant remanent strains of equal and opposite values are used to reversibly and permanently reorient the magnetization state of the Ni film. These experimental results are integrated into micromagnetic simulation to demonstrate the usefulness of this approach for magnetoelectric based magnetic random access memory. © 2011 American Institute of Physics. [doi:10.1063/1.3605571]

Magnetic random access memory (MRAM) is a potential candidate for the next generation of high density memory technologies.¹ Magnetic tunnel junction (MTJ) (Ref. 2) is a viable approach to read data; however, the ability to electrically write non-volatile bit information still remains the major issue. Recently researchers have suggested using magnetoelectric (ME) materials to electrically control magnetization reorientation (i.e., write data) via coupling between magnetic and ferroelectric order parameters.^{3–12} Hu and Nan¹³ and Pertsev and Kohlstedt¹⁴ presented concepts for designing a magnetoelectric magnetic random access memory (ME-MRAM) deposited onto a ferroelectric substrate. The writing consists of reorienting the magnetization direction by 90° using the strain induced by the ferroelectric layer coupled with the magnetocrystalline anisotropy of the ferromagnetic layer to switch between two stable magnetic states. The concept seems plausible and promising; however, experimental results have not been reported.

Recently, Wu *et al.*¹¹ experimentally demonstrated an electric field induced reversible and permanent transition from a magnetic isotropic easy plane to an uniaxial magnetic anisotropy in Ni/(011) $[\text{Pb}(\text{Mg}_{1/3}\text{Nb}_{2/3})\text{O}_3]_{(1-x)}\text{-}[\text{PbTiO}_3]_x$ (PMN-PT, $x \approx 0.32$) ME heterostructure. However, the magnetization states (i.e., one easy plane and one easy axis) did not provide two uniaxial easy axes 90° apart, which is desired for writing/storing bit information. In this paper, we extend the approach and report a magnetoelectric Ni/PMN-PT heterostructure providing two electrically reversible and permanent (metastable) magnetic easy axes. An initial magnetoelastic anisotropy in Ni film (i.e., a preferred easy axis) is achieved by first partially poling the (011) PMN-PT substrate to generate a specific remanent strain prior to Ni film deposition. Reorientation of the magnetic easy axis is achieved by taking advantage of the large anisotropic strain hysteresis properties. Within the context of a ME-MRAM device, a micromagnetic simulation is subsequently used to design a nanoscale magnetic single domain showing that the

two remanent strains produced by PMN-PT substrate are sufficient to achieve electric-field-induced 90° magnetization reorientation.

Prior to the Ni film deposition, the 0.5 mm thick PMN-PT substrate was electro-mechanically characterized to determine the required electric field to produce a specific remanent strain, i.e., half way between the maximum strains produced by the PMN-PT. Figure 1 provides experimental strains of PMN-PT as a function of different bipolar electric fields ($\epsilon\text{-}E$). In these plots, only the strain along the y direction is presented since the x strain response is substantially smaller.^{11,15} Similar to the previous report by Wu *et al.*,¹¹ two giant strain jump peaks are present in the ± 0.42 MV/m curve as well as a giant strain hysteresis is present in the ± 0.14 MV/m curve. For the ± 0.14 MV/m curve, two stable remanent strain states exist (points 1 and 2) defining a critical electric field E_{cr} (-0.14 MV/m) at which the remanent strain is maximized. The giant remanent strains arise from non-180° polarization rotations of $\langle 111 \rangle$ variants from out-of-plane to $x\text{-}y$ in-plane direction.¹⁵ The polarization state at point 1 consists of a $\langle 111 \rangle$ polarization variant mainly aligned in the $x\text{-}y$ plane (illustration 1), while the polarization state at point 2 consists of $\langle 111 \rangle$ variants closest to the z direction (illustration 2). If the electric field is cycled at values larger than E_{cr} (e.g., ± 0.3 MV/m curve) and subsequently removed such that the remanent strain is present as defined by point 3 in Fig. 1, the polarization state consists of a combination of $\langle 111 \rangle$ variants aligned in-plane and $\langle 111 \rangle$ variants diametrically opposed to the original poling direction. On the other hand, if the electric field is cycled at values smaller than E_{cr} (e.g. ± 0.10 MV/m curve) and subsequently removed such that the remanent strain is at point 4, the polarization state consists of a combination of $\langle 111 \rangle$ variants aligned in-plane and $\langle 111 \rangle$ variants close to the original poling direction. These two electric cycling approaches produce a partially poled ferroelectric substrate with a remanent strain (points 3 and 4) half way between the maximum and minimum values (points 1 and 2). However, while the induced remanent strain

^{a)}Electronic mail: charlywu@ucla.edu.

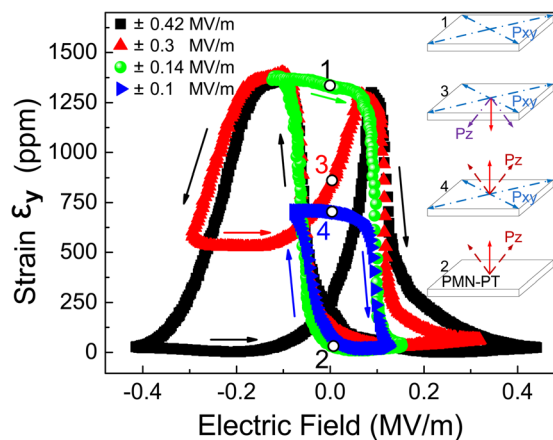


FIG. 1. (Color online) Piezoelectric strain response of (011) PMN-PT along y direction under different bipolar sweeping electric fields. The drawing shows the sample configuration and the coordinate. The arrows indicate the directions of the bipolar electric fields.

is relatively equivalent (points 3 and 4), the crystallographic orientations of the variants are different. To avoid depolarization, we choose the ± 0.1 MV/m partial poling to induce a specific remanent strain prior to Ni deposition in this manuscript.

Once the remanent strain state (point 4 in Fig. 1) is produced, a 5 nm Ti and a 35 nm Ni thin films are deposited onto the PMN-PT sample. Figure 2 shows the measured anisotropic strain $\varepsilon_y - \varepsilon_x$ generated in the Ni film as a function of applied electric fields. Note that point A in Fig. 2 corresponds to point 4 in Fig. 1. The initial point A is defined as the zero strain of the as deposited Ni film. When a positive electric field of 0.14 MV/m is applied and released (points B to C), approximately -700 ppm anisotropic compressive strain (point C) is produced in the Ni film. By applying and releasing a -0.14 MV/m electric field (from point C to points D and E), the PMN-PT substrate undergoes a giant strain jump¹¹ and produces approximately $+700$ ppm anisotropic tensile strain (point E) in the Ni film. As shown in Fig. 2, cycling the electric field between ± 0.14 MV/m switches the remanent anisotropic strain state of Ni/PMN-PT back and forth between -700 ppm compressive and $+700$ ppm tensile. Therefore, the strain induced in the Ni film can be reversibly and perma-

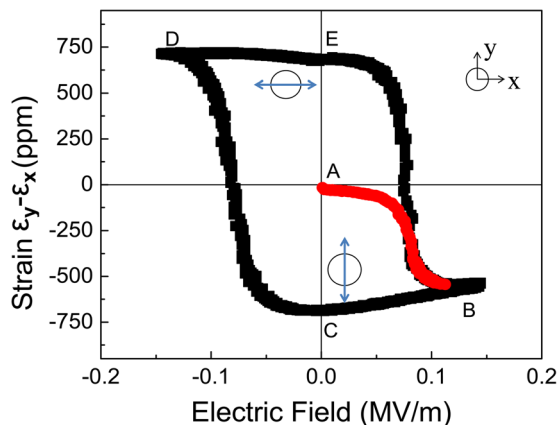


FIG. 2. (Color online) Piezoelectric strain difference $\varepsilon_y - \varepsilon_x$ as a function of applied electric field within $\pm E_{cr}$. The initial point A is defined as the strain free state of as deposited Ni film. The loop B-C-D-E-B shows a complete strain hysteresis. The drawings indicate the magnetization state: (B) and (C) easy axis along y , (D) and (E) easy axis along x .

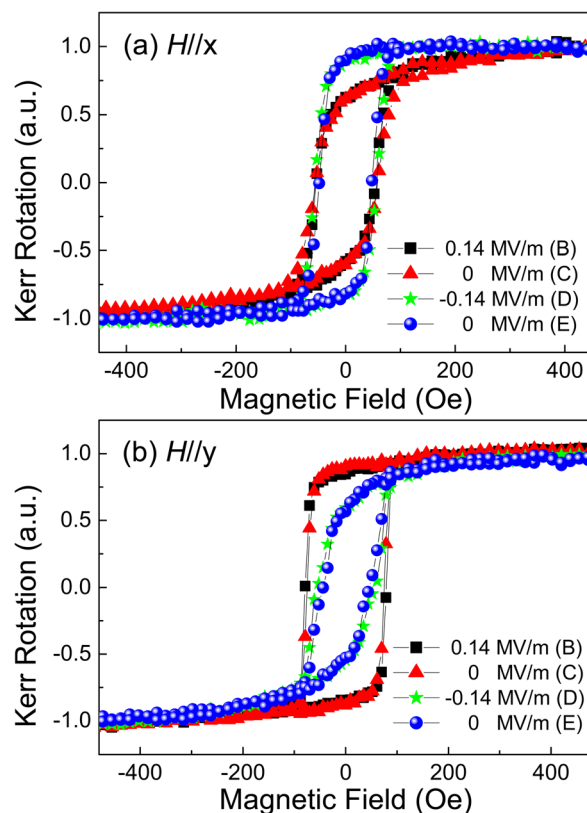


FIG. 3. (Color online) Normalized Kerr rotation hysteresis curves ($M-H$) along (a) x direction and (b) y direction under different electric fields (Letters are the representative of the labeled strain states of the hysteresis loop in the Fig. 2.)

nently switched between two stable remanent strain states (points C and E) of equal and opposite magnitudes.

Figures 3(a) and 3(b) show the normalized Kerr hysteresis curves ($M-H$) of the Ni film on the PMN-PT substrate. Magnetic measurements are performed along both x and y directions for four constant electric fields. All of the constant electric fields are within the strain hysteresis loop B-C-D-E-B as shown in Fig. 2. The compressive strains (points B and C) applied on the Ni film induce an initial magnetoelastic anisotropy aligned along the y direction as seen in Figs. 3(a) and 3(b). The normalized remanent magnetization M_r/M_s in curves B and C are greater than 0.9 along y while below 0.7 along x . By applying a -0.14 MV/m electric field to the sample and releasing it, the strain state of Ni film switches from compressive to tensile along the y direction, which reorients the magnetic anisotropy from y to x as seen in curves D and E of Figs. 3(a) and 3(b). Since the two remanent strain states at points C and E are reversible and stable, the magnetic easy axis of Ni film can be reversibly and permanently switched between two stable magnetic easy axes perpendicular to each other.

Although our experimental data indicate that the magnetization of a thin film ME heterostructure can be electrically switched between two stable perpendicular magnetic easy axes, numerous specifications related to the development of a MEMRAM are required, including (i) a single domain magnetization state to store the bit information and (ii) a magnetic energy barrier for each magnetization state for thermal stability. Here, we use a commercial LLG Micromagnetic Simulator¹⁶ to demonstrate a possible circular nanodisk design that satisfies both mentioned requirements assuming the remanent strains in Fig. 2.

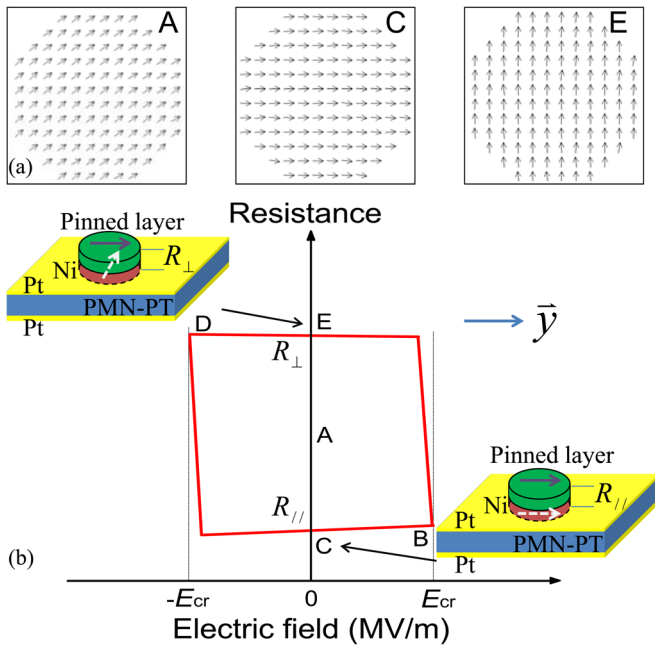


FIG. 4. (Color online) (a) Magnetic single domain configurations of an 80 nm diameter 8 nm thick Ni nanodisk under applied strains of 0 ppm (A), -700 ppm (C), and $+700$ ppm (E), computed from micromagnetic simulation; (b) A hysteresis loop of the TMR as a function of applied electric field accompanied with the magnetization switching.

The equilibrium magnetization results from the minimization of the free energy by incorporating the strain-induced magnetic anisotropy into the free energy.¹⁷ Fig. 4(a) shows the simulated magnetic domain states for an 80 nm diameter and 8 nm thick ($80 \text{ nm} \times 8 \text{ nm}$) Ni nanodisk structure under three different remanent strain states shown in Fig. 2, i.e., (1) 0 ppm (point A), (2) $+700$ ppm (point E), and (3) -700 ppm (point C). Fig. 4(a) illustration A shows that the Ni nanodisk is a single domain in the absence of strain. The illustrations C and E indicate that the application of ± 700 ppm strains causes the nanodisk to reorient its magnetization by 90° . Therefore, by electrically cycling the strain between points C and E, a single domain state can be permanently reoriented by 90° . The magnetic anisotropy of points C and E is calculated to be $K_{\text{eff}} = 5 \times 10^4 \text{ erg/cm}^3$. Therefore, the energy barrier ratio for this particular volume at room temperature is $K_{\text{eff}} V / K_b T \approx 50$, which is sufficient to satisfy the thermal stability criteria suggested for ME-MRAM applications.¹⁸

Fig. 4(b) illustrates the change in tunneling magnetoresistance (TMR) as a function applied electric field within $\pm E_{cr}$ for a ME-MRAM device with a patterned MTJ unit on top of the (011) PMN-PT/Ni nanodisk. Since the magnetization of the Ni nanodisk is a function of the remanent strain state (points C or E), the TMR shows a minimum value $R_{//}$ when the pinned layer and free layer have the same magnetization direction (point C) and a maximum R_{\perp} when the magnetization direction of the free layer rotates perpendicular to the pinned layer. Since the magnetization direction of the free layer is defined by the pinned layer (i.e., $+y$ -direction) at point C, the TMR shows a minimum value $R_{//}$. When a negative electric field $-E_{cr}$ is applied and released (point E), the magnetization direction of the free layer rotates by 90° away from the pinned layer (i.e.,

x -direction) and the TMR shows a maximum value R_{\perp} . Due to the uniaxial nature of the magnetoelastic anisotropy, one of the two possible magnetization directions either $+90^\circ$ or -90° takes place with equal probability. In both cases, the TMR has the same value, since the TMR depends on the absolute value of the angle difference between the pinned and free layers. Please note that the energy influence from pinned layer is ignored, but the contribution can be compensated by properly engineering the initial prestress. By applying and releasing the electric field at $\pm E_{cr}$, two perpendicular magnetic single domain states are switched and retained. Therefore, our simulation supports that non-volatile bit information “0” or “1” can be written by a low electrical energy and read by measuring the TMR.

In summary, we have demonstrated a Ni/PMN-PT ME heterostructure providing an electric-field-induced switching between two reversible and permanent magnetic easy axes perpendicular to each other. The tunable remanent strain defines the initial magnetoelastic anisotropy while the giant strain hysteresis reversibly and permanently reorients the magnetization state. This experimental data were used to design a ME-MRAM with MTJ unit for information storage. This magnetoelectric memory approach provides a promising technology for spintronics and MRAM applications.

This work was partially supported by the Air Force Office of Scientific Research (AFOSR) under Grant No. FA9550-09-1-0677 managed by Byung-Lip (Les) Lee, the Swiss National Science Foundation (SNF) under Grant No. PBNEP2-124323, and the DARPA Non-Volatile Magnonic Logic (NVL) Project under Contract No. HR0011-10-C-0153.

¹J. G. Zhu, *Proc IEEE* **96**(11), 1786 (2008).

²M. Bibes and A. Barthelemy, *Nature Mat.* **7**(6), 425 (2008).

³C.-W. Nan, M. I. Bichurin, S. X. Dong, D. Viehland, and G. Srinivasan, *J. Appl. Phys.* **103**(3), 031101 (2008).

⁴J. F. Scott, *Nature Mat.* **6**(4), 256 (2007).

⁵F. Zavaliche, T. Zhao, H. Zheng, F. Straub, M. P. Cruz, P. L. Yang, D. Hao, and R. Ramesh, *Nano Lett.* **7**(6), 1586 (2007).

⁶Y.-H. Chu, L. W. Martin, M. B. Holcomb, M. Gajek, S.-J. Han, Q. He, N. Balke, C.-H. Yang, D. Lee, W. Hu, Q. Zhan, P.-L. Yang, A. Fraile-Rodriguez, A. Scholl, S. X. Wang, and R. Ramesh, *Nature Mat.* **7**(6), 478 (2008).

⁷M. Liu, O. Obi, J. Lou, Y. Chen, Z. Cai, S. Stoute, M. Espanol, M. Lew, X. Situ, K. S. Ziemer, V. G. Harris, and N. X. Sun, *Adv. Funct. Mater.* **19**(11), 1826 (2009).

⁸M. Liu, O. Obi, Z. Cai, J. Lou, G. Yang, K. S. Ziemer, and N. X. Sun, *J. Appl. Phys.* **107**(7), 073916 (2010).

⁹Z. Li, J. Wang, Y. Lin, and C. W. Nan, *Appl. Phys. Lett.* **96**(16), 162505 (2010).

¹⁰T. Wu, A. Bur, J. L. Hockel, K. Wong, T. Chung, and G. P. Carman, *IEEE Magn. Lett.* **2**, 6000104 (2011).

¹¹T. Wu, A. Bur, P. Zhao, K. P. Mohanchandra, K. Wong, K. L. Wang, C. S. Lynch, and G. P. Carman, *Appl. Phys. Lett.* **98**(1), 012504 (2011).

¹²T. Wu, A. Bur, K. Wong, J. L. Hockel, C.-J. Hsu, H. K. D. Kim, K. L. Wang, and G. P. Carman, *J. Appl. Phys.* **109**(7), p. 07D732 (2011).

¹³J.-M. Hu and C. W. Nan, *Phys. Rev. B* **80**(22), 224416 (2009).

¹⁴N. A. Pertsev and H. Kohlstedt, *Appl. Phys. Lett.* **95**(16), 163503 (2009).

¹⁵T. Wu, P. Zhao, M. Bao, A. Bur, J. L. Hockel, K. P. Mohanchandra, C. S. Lynch, and G. P. Carman, *J. Appl. Phys.* **109**(12), 124101 (2011).

¹⁶M. Scheinfein and E. Price, in <http://llgmicro.home.mindspring.com/>.

¹⁷A. Bur, T. Wu, J. L. Hockel, C.-J. Hsu, H. K. D. Kim, T.-K. Chung, K. Wong, K. L. Wang, and G. P. Carman, *J. Appl. Phys.* **109**(12), 123903 (2011).

¹⁸B. Cullity and C. Graham, *Introduction to Magnetic Materials*. (Wiley-IEEE, Hoboken, NJ, 2008).